Unravelling the complexity and redundancy of carbon catabolic repression in *Pseudomonas fluorescens* SBW25

Yunhao Liu,[1,2†] Chaitanya S. Gokhale,[2,4]
Paul B. Rainey[2,3,5] and Xue-Xian Zhang [ID][1]*
[1]*Institute of Natural and Mathematical Sciences, Massey University at Albany, Auckland 0745, New Zealand.*
[2]*New Zealand Institute for Advanced Study, Massey University at Albany, Auckland 0745, New Zealand.*
[3]*Department of Microbial Population Biology, Max Planck Institute for Evolutionary Biology, Plön 24306, Germany.*
[4]*Department of Evolutionary Theory, Max Planck Institute for Evolutionary Biology, Plön 24306, Germany.*
[5]*Ecole Supérieure de Physique et de Chimie Industrielles de la Ville de Paris (ESPCI ParisTech), CNRS UMR 8231, PSL Research University, 75231 Paris Cedex 05, France.*

Summary

The two-component system CbrAB is the principal regulator for cellular metabolic balance in *Pseudomonas fluorescens* SBW25 and is necessary for growth on many substrates including xylose. To understand the regulatory linkage between CbrAB and genes for xylose utilization (*xut*), we performed transposon mutagenesis of ∆*cbrB* to select for Xut⁺ suppressors. This led to identification of *crc* and *hfq*. Subsequent genetic and biochemical analysis showed that Crc and Hfq are key mediators of succinate-provoked carbon catabolite repression (CCR). Specifically, Crc/Hfq sequentially bind to mRNAs of both the transcriptional activator and structural genes involved in xylose catabolism. However, in the absence of succinate, repression is relieved through competitive binding by two ncRNAs, CrcY and CrcZ, whose expression is activated by CbrAB. These findings provoke a model for CCR in which it is assumed that *crc* and *hfq* are functionally complementary, whereas *crcY* and *crcZ* are genetically redundant. Inactivation of either *crcY* or *crcZ* produced no effects on bacterial fitness in laboratory media, however, results of mathematical modelling predict that the co-existence of *crcY* and *crcZ* requires separate functional identity. Finally, we provide empirical evidence that CCR is advantageous in nutrient-complex environments where preferred carbon sources are present at high concentrations but fluctuate in their availability.

Introduction

Carbon catabolite repression (CCR) allows bacteria to acclimate rapidly to preferred carbon and energy sources thereby maximizing growth rate. The classic example comes from *Escherichia coli*, which preferentially utilizes glucose over lactose when both are present: transcription of lactose utilization (*lac*) genes is activated by the catabolite-activating protein (CAP) charged with cAMP, but adenylate cyclase for cAMP synthesis (and lactose transporter) is inhibited in the presence of glucose (Deutscher, 2008; Goerke and Stulke, 2008). However, this well-defined paradigm does not hold for many non-enteric bacteria, including those of the closely related genus *Pseudomonas* (Collier *et al.*, 1996; Rojo, 2010). Pseudomonads are metabolically versatile but use succinate as one of the preferred carbon sources. Succinate inhibits the expression of many transporter and catabolic genes such as those for the utilization of histidine, glucose, and mannitol (MacGregor *et al.*, 1991; Hester *et al.*, 2000). The *Pseudomonas* genome does contain a CAP homologue termed Vfr, but it plays no role in CCR (Suh *et al.*, 2002). Moreover, intracellular levels of cAMP remain unchanged in the presence and absence of succinate (Phillips and Mulfinger, 1981).

In the early 1990s the first insights into CCR in *P. aeruginosa* became apparent. Using chemical mutagenesis and enrichment procedures, Wolff and coworkers (1991) identified mutants capable of utilizing lactamide in the presence of succinate. These CCR⁻ mutants led to identification of *crc* whose amino acid sequence shows low, but significant similarity to exo-deoxyribonuclease III; however, no DNA or RNA

nuclease activities have been detected for Crc proteins from *P. aeruginosa* or *P. putida* (MacGregor *et al.*, 1996; Ruiz-Manzano *et al.*, 2005). Consequently, until recently, the precise role of Crc in CCR remained unclear (Rojo, 2010). The current model – derived from studies of *P. aeruginosa*, *P. putida* and *P. syringae* – shows that CCR occurs at the post-transcriptional level, and is mediated by complex interactions among multiple regulatory components (Sonnleitner *et al.*, 2009; Hernandez-Arranz *et al.*, 2013; Filiatrault *et al.*, 2013). These include the abovementioned Crc, a RNA chaperonic protein Hfq, a two-component regulatory system CbrA/CbrB, as well as non-coding RNAs (ncRNAs) such as CrcZ. When substrate-specific catabolic genes are transcriptionally induced, translation is repressed by the RNA-binding proteins Crc/Hfq in the presence of succinate. When succinate is consumed, the Crc/Hfq protein complex is sequestered by ncRNAs whose expression is activated by CbrAB. While key components of CCR have been identified, critical details are still lacking regarding molecular interactions between Crc and Hfq as well as RNA targeting. It is also difficult to understand why *Pseudomonas* strains have evolved such a complex CCR system, particularly the involvement of multiple ncRNAs. For example, three copies of CbrAB-regulated ncRNAs are involved in sequestration of the Crc/Hfq complex in *P. syringae* (Filiatrault *et al.*, 2013). The reasons for such redundancy are unknown. Also not understood are the ecological conditions under which CCR contributes a fitness advantage.

Here, we describe CCR in the plant growth-promoting bacterium *P. fluorescens* SBW25 (Silby *et al.*, 2009; Rainey and Bailey, 1996). Our work specifically focuses on succinate-induced repression of *xut* genes for xylose utilization. Xylose is the backbone monomer of hemicellulose, which is a major structural component of the plant cell wall. Monomeric xylose is water-soluble, and exists in various natural environments, such as soil and the digestive tract of higher animals (Shallom and Shoham, 2003). Interestingly, for currently unknown physiological reasons, xylose also accumulates on the surfaces of plants, and has been identified as a dominant constituent of root exudates in a wide range of plant species (Dakora and Phillips, 2002). Many plant-associated bacteria such as *P. fluorescens* SBW25 are capable of growth on xylose as a source of carbon and energy (Zhang and Rainey, 2008; Liu *et al.*, 2015).

A key enzyme for xylose catabolism is the xylose-specific isomerase (XutA). It converts xylose to xylulose, which is then phosphorylated to produce xylulose-5-phosphate (xylulose-5-P), an intermediate of the pentose phosphate pathway. In a previous work, we showed that the *xutA* gene is co-transcribed with *xutFGH*, which encodes an ABC-type transporter system for xylose

uptake (Liu *et al.*, 2015). Transcription of the *xutAFGH* operon is regulated by a divergently organised AraC-type activator (XutR) in a xylose-dependent manner. Intriguingly, the *xut* locus is expressed at elevated levels during the process of bacterial colonization on the surfaces of sugar beet, from where *P. fluorescens* SBW25 was originally isolated (Rainey, 1999). We previously showed that the two-component regulatory system CbrA/CbrB plays an important role in the coordinate expression of genes for nutrient utilization in *P. fluorescens* SBW25. A mutant devoid of *cbrB* is compromised in the ability to utilize a wide range of nutritional substrates, including xylose (Zhang and Rainey, 2007, 2008). However, extensive characterization of the *xutAFGH* promoter region (P_A) revealed no evidence of direct CbrB-binding to the P_A promoter DNA (Liu *et al.*, 2015). This suggested that the effects of CbrB on *xut* gene expression might be mediated by as-yet-unidentified factors in the CbrAB regulon.

This study began with mutagenesis of $\Delta cbrB$ (Xut⁻) with the aim of selecting suppressor mutants that grow on xylose (Xut⁺). This led to the identification of *crc* and *hfq* genes, which are required for CbrAB regulation of xylose utilization. Given the established role of *crc* in CCR control in other *Pseudomonas* species, we then focused on the molecular mechanisms of CCR in *P. fluorescens* SBW25. A combination of genetic and biochemical approaches reveal complex molecular interactions between Crc and Hfq, which target mRNA transcripts of all three genetic components for xylose utilization (i.e. *xutA*, *xutFGH* and *xutR*). We identified two CbrAB-regulated ncRNAs (namely, CrcY and CrcZ) involved in the sequestration of Crc/Hfq. Significantly, we show that CrcY and CrcZ are functionally redundant: deletion of either *crcY* or *crcZ* did not cause a decrease of bacterial fitness in laboratory media. However, our results of mathematical modelling led to the hypothesis that the redundant gene must possess different biological functions for its maintenance. Finally, we provide empirical evidence regarding the nutrient conditions under which CCR confers an ecological advantage.

Results

Identification of xylose-utilising mutants of ΔcbrB

To identify the predicted unknown activators of the *xutAFGH* operon, we adopted a transposon (Tn) mutagenesis strategy to select for $\Delta cbrB$ mutants (which are phenotypically Xut⁻) that grow on xylose as the sole source of carbon and energy. The suppressor analysis was performed with IS-Ω-Km/hah, which harbours an outward promoter at one end and thus can drive expression of cryptic activators (Giddens *et al.*, 2007). Twenty
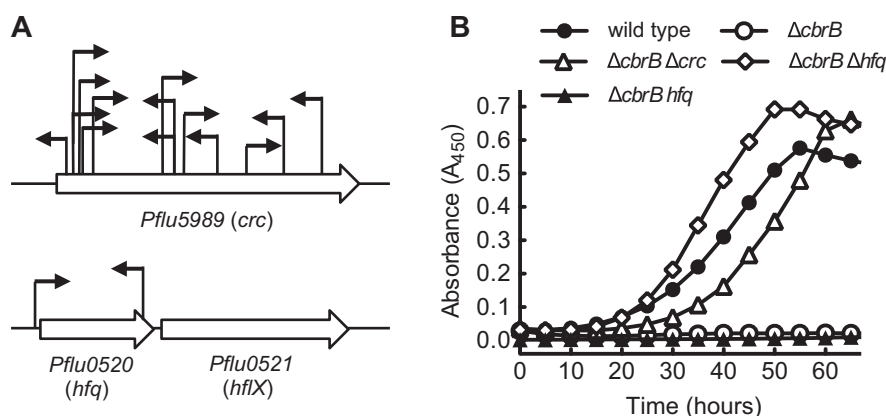
Fig. 1. Genetic identification of Crc and Hfq in CbrB-mediated regulatory control of xylose utilization in *P. fluorescens* SBW25.
A. Locations of Tn insertions in the 16 Xut$^+$ suppressors of ΔcbrB. Bent arrows denote the location of IS-Ω-Km/hah and orientation of the *nptII* promoter carried in the transposon.
B. Growth dynamics of wild-type SBW25 and mutants PBR810 (ΔcbrB), MU47–12 (ΔcbrB Δcrc), MU47–13 (ΔcbrB Δhfq) and MU47–19 (ΔcbrB hfq over-expression). Bacteria were grown in minimal salts medium supplemented with xylose (20 mM) as the sole carbon source. Data are means and standard errors for five independent cultures.

Xut$^+$ mutants were randomly picked from selective agar plates of M9 salt medium supplemented with xylose and nitrofurantoin (to counter select *E. coli*) and kanamycin (Km). Next, the genomic locations of the Tn insertions were determined using an arbitrary-primed PCR (AP-PCR) strategy followed by DNA sequencing. A total of sixteen mutants were successfully mapped and no putative activator genes were identified: fourteen mapped to the coding region of Crc, and two to the *hfq* locus (Fig. 1A). Tn insertions in *crc* were scattered across the coding region, indicative of loss-of-function mutations. However, for the two *hfq* mutants one carries the Tn close to the 3'-end of the coding region and the other harbours the Tn in the putative ribosomal binding site of *hfq*, suggesting that suppression might be caused by either a loss-of-function mutation or overexpression of *hfq*.

To further verify the results of the Tn analysis, double deletion mutants of ΔcbrB Δcrc and ΔcbrB Δhfq were constructed by site-directed mutagenesis. Additionally, the *hfq* coding region was cloned into the mini-Tn7 vector pUC18-mini-Tn7T-LAC and introduced into the genome of the ΔcbrB mutant. The three mutants were then subjected to growth assay on xylose as the sole carbon source (Fig. 1B, Table 1). Results show that deletion of either *crc* or *hfq*, but not *hfq* overexpression, restored the ability of the ΔcbrB mutant to grow on xylose. Together, the data show that CbrAB-mediated activation of the *xut* locus is achieved via de-repression of Crc and Hfq.

Identification of two ncRNAs in the regulation of xut *genes expression*

Crc has long been known as a mediator of CCR in *Pseudomonas*, whereas at the time this work was performed Hfq was known as a general small RNA chaperonic protein with no known role in CCR. On the basis of the Tn analysis described above and available evidence (Sonnleitner *et al.*, 2009; Moreno *et al.*, 2009b), we predicted that Crc represses expression of *xut* genes, and that such repression holds even when CbrB is inactivated.

In *P. aeruginosa* it has been shown that CbrB activates expression of a non-coding RNA termed CrcZ, which de-represses Crc activity (Sonnleitner *et al.*, 2009). If the same holds for *P. fluorescens* SBW25, a Xut$^-$ phenotype should be associated with the ΔcrcZ mutant (as observed in *P. aeruginosa* for other CbrB-regulated catabolic genes [NB, *P. aeruginosa* cannot utilize xylose]). In previous work we showed that *crcZ* encodes a non-coding RNA under the control of CbrAB, but also showed that a *crcZ* deletion mutant manifests none of the growth defects observed for the ΔcbrB mutant, including xylose utilization (Zhang *et al.*, 2010). Interrogation of the SBW25 genome led to identification of a *crcZ* homologue located in the intergenic region between *pflu3887* and *pflu3888* (termed *crcY*). Thus, we predicted that CrcY and CrcZ are functionally redundant; and that *crcY* would thus complement the *crcZ* gene deletion. Indeed, the double deletion mutant of *crcY* and *crcZ* (strain MU34–61) showed no growth on xylose; in the contrast, mutants devoid of either *crcY* or *crcZ* grew normally on xylose (Supporting Information Fig. S1A).

Next we asked if *crcY* and *crcZ* are both regulated by CbrAB. We have previously shown that *crcZ* is transcribed from a σ^{54}-type promoter (P$_{crcZ}$) and that deletion of *cbrB* compromised P$_{crcZ}$ promoter activity (Zhang *et al.*, 2010). First, to gain insight into the CbrB operator site, transcriptional *lacZ* fusions were constructed (in the

Table 1. Bacterial strains and plasmids used in this work.

Strain or plasmid	Genotypes and relevant characteristics	Reference
P. fluorescens		
SBW25	Wild-type strain isolated from phyllosphere of sugar beet, Xut$^+$	Bailey *et al.* (1995)
PBR810	Δ*cbrB*, SBW25 devoid of *pflu5237*, Xut$^-$	Zhang and Rainey (2007)
MU12–58	Δ*crc*, SBW25 devoid of *pflu5989*, Xut$^+$	This work
MU47–11	Δ*hfq*, SBW25 devoid of *pflu0520*, Xut$^+$	This work
MU47–12	Δ*crc* Δ*cbrB*, SBW25 with the deletion *pflu5989* and *pflu5237*, Xut$^+$	This work
MU47–13	Δ*hfq* Δ*cbrB*, SBW25 with the deletion *pflu0520* and *pflu5237*, Xut$^+$	This work
MU47–19	SBW25Δ*cbrB* carrying mini-Tn7T-LAC::*hfq*, Xut$^-$	This work
MU30–34	SBW25Δ*crcZ*, Xut$^+$	This work
MU34–64	SBW25Δ*crcY*, Xut$^+$	This work
MU34–61	SBW25Δ*crcZ* Δ*crcY*, Xut$^-$	This work
MU47–17	SBW25Δ*crc* Δ*crcZ* Δ*crcY*, Xut$^+$	This work
Plasmid		
pCR8/GW/TOPO	Cloning vector, Sp^r	Invitrogen
pRK2013	Helper plasmid, Tra$^+$, Km^r	Ditta *et al.* (1980)
pSCR001	Plasmid carrying the IS-Ω-Km/hah element, Km^r	Giddens *et al.* (2007)
pUC18-mini-Tn7T-LAC	Mini-Tn7 vector, Ap^r, Gm^r	Choi *et al.* (2005)
pUC18-mini-Tn7T-Gm-*lacZ*	Mini-Tn7 vector for transcriptional fusion to promoterless *lacZ*, Ap^r, Gm^r	Choi *et al.* (2005)
pXY2	Mini-Tn7 vector for a *lacZ* translational fusion, Ap^r, Gm^r	Liu *et al.* (2014)
pUX-BF13	Helper plasmid for transposition of mini-Tn7 element, Ap^r	Bao *et al.* (1991)
pXY2-P$_{crc}$	pXY2 containing the P$_{crc}$-*lacZ* translational fusion, Ap^r, Gm^r	This work
pXY2-P$_{hfq}$	pXY2 containing the P$_{hfq}$-*lacZ* translational fusion, Ap^r, Gm^r	This work
pXY2-P$_R$	pXY2 containing a translational *lacZ* fusion to the P$_R$ promoter for *xutR* expression	This work
pXY2-P$_A$	pXY2 containing a translational *lacZ* fusion to the P$_A$ promoter for *xutAFGH* expression	This work
pXY6-*hfq*	pUC18-mini-Tn7T-LAC containing *hfq* for over-expression	This work
pXY7-P$_R$	pUC18-mini-Tn7T-*lacZ* containing a transcriptional *lacZ* fusion to the P$_R$ promoter for *xutR* expression	Liu *et al.* (2015)
pXY7-P$_A$	pUC18-mini-Tn7T-*lacZ* containing a transcriptional *lacZ* fusion to the P$_A$ promoter for *xutA* expression	Liu *et al.* (2015)
pXY7-P$_Z$1	pUC18-mini-Tn7T-*lacZ* containing *lacZ* fusion to P$_Z$ promoter for *crcZ* (-264 to +100)	This work
pXY7-P$_Z$2	pUC18-mini-Tn7T-*lacZ* containing *lacZ* fusion to P$_Z$ promoter for *crcZ* (-153 to +100)	This work
pXY7-P$_Z$3	pUC18-mini-Tn7T-*lacZ* containing *lacZ* fusion to P$_Z$ promoter for *crcZ* (-88 to +100)	This work
pUIC3	Suicide vector with promoterless '*lacZ*, Mob$^+$, Tc^r	Rainey (1999)
pUIC3–42	pUIC3 containing *cbrA-lacZ* fusion, Tc^r	Zhang and Rainey (2008)
pUIC3–43	pUIC3 containing *cbrB-lacZ* fusion, Tc^r	Zhang and Rainey (2008)
pUIC3–65	pUIC3 containing *crcZ-lacZ* fusion, Tc^r	Zhang *et al.* (2010)
pUIC3–152	pUIC3 containing *crcY-lacZ* fusion, Tc^r	This work
pTrc99A	Protein expression vector, P$_{tac}$ promoter, Ap^r	Amann *et al.* (1988)
pTrc99A-*crc*	pTrc99A carrying Crc$_{His6}$, Ap^r	This work
pTrc99A-*hfq*	pTrc99A carrying Hfq$_{His6}$, Ap^r	This work

mini-Tn7 vector) to three P$_{crcZ}$ fragments with the same 3′-end but with a variable 5′-end from residue −264, −153 and −88, respectively (Supporting Information Fig. S2). Results of β-galactosidase assay showed that a 64 bp DNA region containing sequence motifs that are homologous to the CbrB binding sequences (as determined *in vitro* in *P. aeruginosa* [Lu *et al.*, 1999]) was required for P$_{crcZ}$ functionality. P$_{crcZ}$ information was then used for *in silico* analysis of the P$_{crcY}$ promoter. As shown in Supporting Information Fig. S2, the P$_{crcY}$ promoter contains putative CbrB-binding sequences that are identical to that of the P$_{crcZ}$ promoter; and moreover, a putative σ^{54}-binding site was also detected. To determine the 5′-end of CrcY, 5′-RACE analysis was performed using total mRNAs prepared from cells grown on minimal medium with xylose as the sole carbon source. Results confirmed the predicted σ^{54}-binding site: transcription starts at the 13th nucleotide downstream from the conserved C residue of the −12 element (Supporting Information Fig. S2B). Finally, to test the requirement of CbrAB for CrcY expression, a transcriptional P$_{crcY}$-*lacZ* fusion was constructed in the genetic backgrounds of wild-type SBW25 and its derived Δ*cbrB* mutant. Consistent with expectation, deletion of *cbrB* abolished P$_{crcY}$ promoter activity (Supporting Information Fig. S2). Together, these data led us to conclude that both CrcY and CrcZ are regulated by the CbrAB system in a σ^{54}-dependent manner.

Data presented thus far show that both $\Delta cbrB$ and $\Delta crcY$ $\Delta crcZ$ mutants are unable to grow on xylose (Xut⁻), and that CbrAB de-represses Crc activity for the expression of *xut* genes [consequently, mutant $\Delta cbrB$ was Xut⁻, whereas the double deletion mutant $\Delta cbrB$ Δcrc was Xut⁺ (Fig. 1B)]. More importantly, CbrAB activates expression of the CrcY and CrcZ small RNAs that have the potential to interact with Crc. These findings cumulatively suggest that the observed CbrAB-dependent Crc de-repression is mediated through CrcY and CrcZ. If this is true, a Xut⁺ phenotype would be expected for a triple deletion mutant of Crc, CrcY and CrcZ. Indeed, when *crc* was deleted in the genetic background of $\Delta crcY$ $\Delta crcZ$ (Xut⁻), it restored the ability to grow on xylose (strain MU47–17, Xut⁺) (Supporting Information Fig. S1B).

Finally, we sought empirical evidence to demonstrate molecular interactions between Crc and CrcY/CrcZ. To this end, His$_6$-tagged Crc from *P. fluorescens* SBW25 was expressed in *E. coli* and the purified proteins were subjected to electrophoretic mobility shift assays (EMSA) using CrcY and CrcZ RNA transcripts that were synthesized *in vitro* with the help of T7 RNA polymerase. Results shown in Supporting Information Fig. S3 implicate specific interactions between Crc protein and the CrcY and CrcZ ncRNAs. However, recent progress has been made in other *Pseudomonas* species, suggesting that Crc does not bind to RNAs *per se*; the *in vitro* Crc$_{His6}$ RNA binding activity was actually conferred by Hfq co-purified from *E. coli* cells (Milojevic *et al.*, 2013a, 2013b; Moreno *et al.*, 2015). This is likely the case for Crc$_{His6}$ of *P. fluorescens* SBW25, which was also prepared from *hfq*⁺ *E. coli* cells. However, all empirical data presented here, particularly the above-described Tn mutagenesis consistently indicate that Crc and Hfq act in a coordinate manner to mediate repression of *xut* genes for xylose utilization.

Effects of alternative carbon source on the expression of xylose utilization genes

Xylose is abundant in nature, but it supports relatively slow bacterial growth. Thus, it makes sense that the expression of *xut* genes is subject to repression by the co-presence of many other carbon substrates. However, the nature of CCR has not been examined in *P. fluorescens* SBW25. To this end, a translational *lacZ* fusion was constructed in the wild-type background to the previously well-characterized P$_A$ promoter of the *xutAFGH* operon. β-Galactosidase activities were measured for cells grown on xylose plus each of 10 other carbon substrates. Data acquired at 6 h after inoculation indicate strong inhibition by succinate, glutamate and glucose,

and weak inhibition by citrate, arabinose and mannitol (Supporting Information Fig. S4A). Significantly, no inhibitory effects were observed for glycerol, histidine, betaine or galactose. The inhibitory effects of succinate and non-inhibitory effects of glycerol were further confirmed by assays of β-galactosidase activities every 2 h over a period of 8 h after inoculation (Supporting Information Fig. S4B and C). Succinate is a preferred carbon source used in previous CCR studies in *Pseudomonas* (Rojo, 2010). Interestingly, glycerol supports rapid bacterial growth with a maximum growth rate (μmax) of 0.853 ± 0.018 per hour, which is comparable to that of succinate (0.855 ± 0.010 per hour) (Supporting Information Fig. S4D). Hereafter, 'xylose plus succinate' and 'xylose plus glycerol' were used as the assay conditions for CCR and non-CCR, respectively. However, it should be noted that the xylose-induced *xutA* gene expression was not abolished by the co-presence of succinate (Supporting Information Fig. S4C). Only a two-thirds reduction of *xutA* gene expression was observed for succinate-provoked CCR (Supporting Information Fig. S4E).

Next, we monitored the expression levels of *xutR* using both transcriptional and translational *lacZ* fusions in the genetic backgrounds of wild-type SBW25 and an isogenic Δcrc mutant. Results of β-galactosidase assays under CCR and non-CCR growth conditions showed that *xutR* was transcribed at similar levels under the four combined genetic and nutrition conditions (Fig. 2A). A significant reduction of *xutR* translation was observed in the presence of succinate in the wild-type background, but not in the Δcrc background (Fig. 2B). These data clearly indicate that the succinate-provoked CCR occurs at the level of translation (not transcription), which can be fully explained by activities of the Crc protein.

Similar work was performed using transcriptional and translational *lacZ* fusions to the *xutA* promoter. The data presented in Fig. 2C indicate that succinate causes a significant reduction of *xutA* transcription in wild type, but not in the Δcrc mutant background. This result is consistent with the fact that the Crc-regulated XutR protein is a transcriptional activator of the *xutAFGH* operon. Notably, a more pronounced succinate-induced repression was detected at the level of translation in wild-type SBW25, and inactivation of Crc caused a significant increase of *xutA* translation under CCR conditions (Fig. 2D). However, contrary to expectation, CCR was not abolished by deletion of *crc*: expression of the P$_A$-*lacZ* translational fusion in the Δcrc mutant background was still significantly lowered by the presence of succinate (Fig. 2D). This implicates the involvement of some yet-unknown CCR regulatory factors.
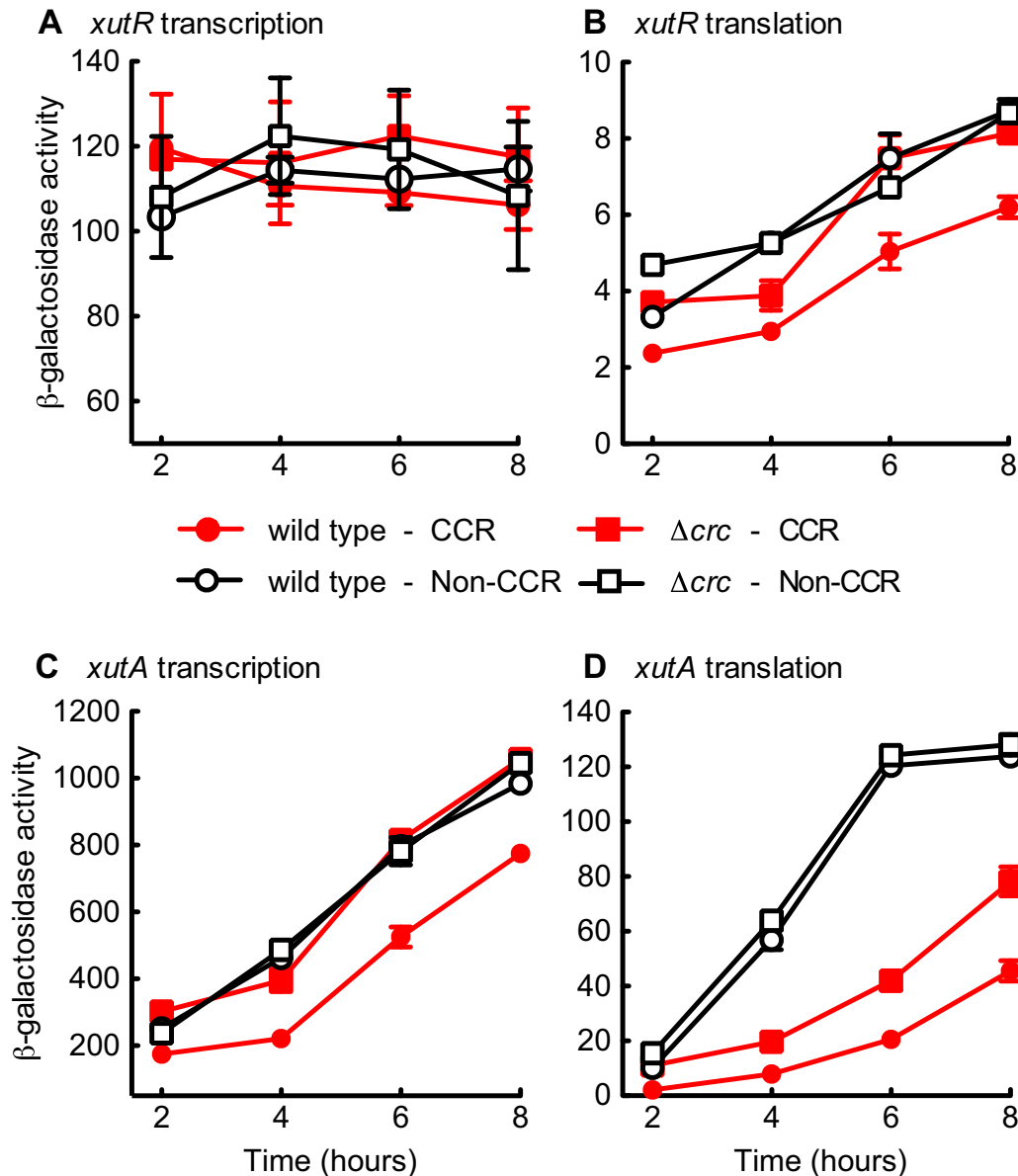
Fig. 2. Levels of transcription and translation of *xutA* and *xutR* genes in wild-type and Δ*crc* backgrounds. Bacteria were grown in minimal salts medium supplemented with 'xylose + succinate' (CCR) or 'xylose + glycerol' (Non-CCR) as the carbon sources. β-Galactosidase activities were measured at 2, 4, 6 and 8 h after inoculation and data are means and standard errors for three independent cultures.

Determining the in vitro *molecular interactions between Crc/Hfq and their target RNAs*

Interrogation of DNA sequences at the *xut* locus revealed a total of five putative Crc/Hfq-binding sites, two of which are located in the vicinity of the translational start site of XutA and XutR, respectively (Supporting Information Fig. S5). Three additional A-rich motifs were found in the DNA region of *xutFGH* genes, which encode an ABC-type transporter co-transcribed with *xutA* in a single mRNA (Supporting Information Fig. S5). Two such putative Crc/Hfq-binding sites are located close to the start codons of *xutF* and *xutH*, respectively,

and the third in the *xutF*-coding region. This finding raised the possibility that the Crc/Hfq protein complex specifically targets the mRNA transcripts of all three genetic components required for xylose utilization, i.e., XutFGH for xylose uptake, XutA for enzymatic breakdown of xylose, as well as the xylose-responsive transcriptional activator XutR.

To test the functionality of these A-rich motifs, we first performed EMSA analysis using the biotin-labelled 5′-end region of *xutA* and *xutR* mRNAs (∼120 nt in length) as a probe. Results with purified Crc_{His6} protein indicate specific bindings for both the *xutA* and the *xutR* mRNA
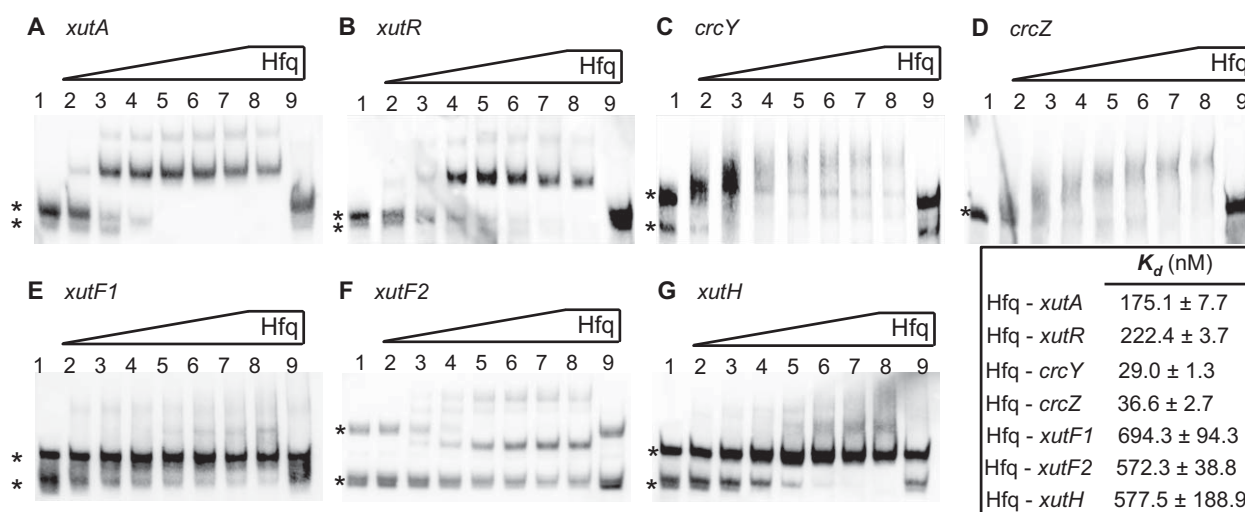
Fig. 3. Specific interactions between Hfq and its target RNAs. Each EMSA experiment was performed using a biotin-labelled RNA probe (0.1 μM) and Hfq$_{His6}$ added at the final concentration of 0, 0.1, 0.2, 0.4, 0.8, 1.2, 1.6, 2.0 and 2.0 μM in lanes 1 to 9, respectively. A 200-fold molar excess of unlabelled probe (competitor RNA) was added in lane 9 as a control for non-specific binding. The protein/RNA samples were separated in native polyacrylamide gels. Asterisks on left-hand side of each gel image denote positions of the free RNA probes. The strength of binding between Hfq and each of the target RNAs is calculated as the equilibrium dissociation constant (K_d) shown at the right bottom corner.

	K_d (nM)
Hfq - *xutA*	175.1 ± 7.7
Hfq - *xutR*	222.4 ± 3.7
Hfq - *crcY*	29.0 ± 1.3
Hfq - *crcZ*	36.6 ± 2.7
Hfq - *xutF1*	694.3 ± 94.3
Hfq - *xutF2*	572.3 ± 38.8
Hfq - *xutH*	577.5 ± 188.9

transcripts. Significantly, mutant mRNAs devoid of the A-rich motifs lost the capability of binding with Crc$_{His6}$ (Supporting Information Fig. S6).

Next, five mRNA fragments of 100–120 nt in length containing each of the five putative Crc/Hfq-binding sties (Supporting Information Fig. S5) were synthesized *in vitro*, and then subject to EMSA analysis with purified Hfq$_{His6}$ protein from *P. fluorescens* SBW25. Results are summarised in Fig. 3. In most cases two bands were detected for the free RNA probes, likely due to the presence of multiple conformations of a RNA molecule. Shifted bands were observed for all five tested RNA fragments; and more importantly, their intensities increased with increased concentrations of Hfq$_{His6}$, coupled with a decrease of free RNA probes (lanes 2–8). The retardation was abolished by adding an excess of the same but unlabelled probe as the specific RNA competitor (lane 9), suggesting that the bindings are specific between Hfq$_{His6}$ and the five target sites in the *xutR* and *xutAFGH* gene transcripts.

Also included in the Hfq$_{His6}$ EMSA analysis were the CrcY and CrcZ ncRNAs, which were produced by *in vitro* transcription. CrcY and CrcZ are of 382 nt and 361 nt in length, respectively. Both contain six putative A-rich motifs for Crc/Hfq binding (Supporting Information Fig. S7). Thus, it was not surprising that they displayed specific high-affinity binding with purified Hfq$_{His6}$ protein (Fig. 3).

On the basis of these EMSA gel images, equilibrium dissociation constants (K_d) between Hfq and the seven target mRNAs were calculated, and the results revealed great variations in the strength of substrate binding

(Fig. 3). Hfq had the highest binding affinities with CrcY and CrcZ (~30 nM), followed by the *xutA* and *xutR* transcripts (~200 nM), and finally, the transporter gene transcripts (*xutF1*, *xutF2* and *xutH* ~600 nM).

Transcriptional responses of CCR regulators to the presence and absence of succinate

Data presented above consistently indicate that the Crc/Hfq complex is the principal mediator of CCR in *P. fluorescens* SBW25 (Fig. 4). Under CCR conditions such as the presence of succinate, Crc/Hfq represses expression of the *xutR* and *xutAFGH* genes through specific binding to five target sites at the two *xut* gene transcripts. When succinate is exhausted, inhibition is relieved via activities of the CbrAB two-component system. CbrAB activates expression of CrcY and CrcZ ncRNAs, which in turn sequester the Crc/Hfq complex and prevent it from binding to the mRNA transcripts of *xut* genes. This model explains the phenotypes observed for the *cbrAB, crcYZ, hfq* and *crc* mutants (Fig. 1 and Supporting Information Fig. S1). Specifically, inactivation of *cbrAB* or *crcYZ* caused no growth on xylose as a result of constant repression of *xut* genes for xylose utilization; and moreover, a secondary mutation either in *crc* or *hfq* restored the ability to use xylose.

To determine the expression levels of CCR regulators under CCR and non-CCR conditions, we constructed *cbrA, cbrB, crcY* and *crcZ* transcriptional *lacZ* fusions, and *crc* and *hfq* translational *lacZ* fusions, in the
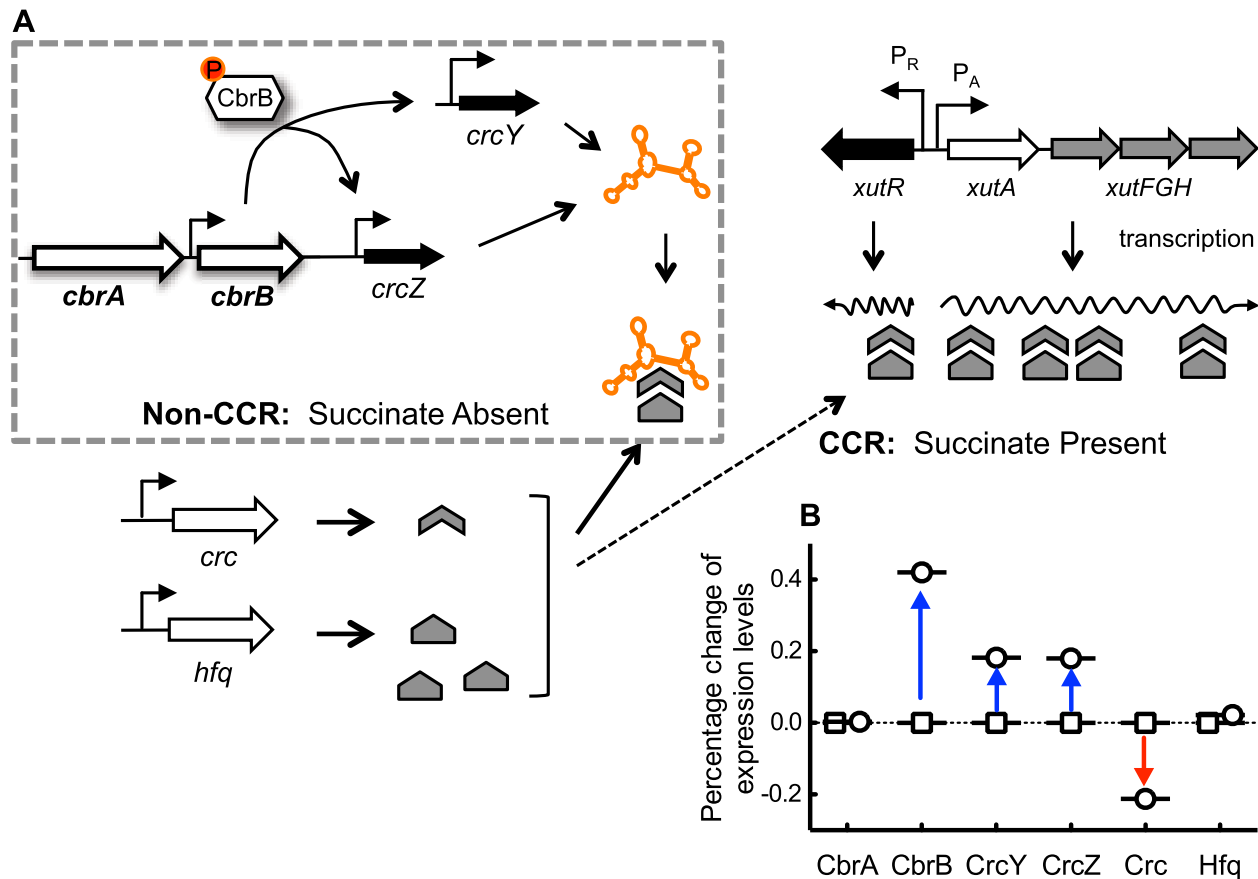
Fig. 4. CCR control of *xut* genes for xylose utilization in *P. fluorescens* SBW25.
A. The Crc/Hfq complex binds to *xutR*, *xutA* and *xutFGH* mRNA transcripts, and consequently, inhibits their translation under CCR conditions such as the presence of succinate. The repression is relieved under Non-CCR conditions via sequestration of the Crc/Hfq complex by CrcY and CrcZ small ncRNAs, whose expression is activated by the CbrAB two-component system.
B. Percentage increase or decrease of expression levels of the CCR regulators during metabolic shift from CCR (square) to Non-CCR (circle) conditions. Bacteria were grown in minimal salt medium supplemented with either 'xylose + glycerol' (Non-CCR) or 'xylose + succinate' (CCR) as the carbon sources. β-Galactosidase activities were measured at 2, 4, 6 and 8 h after inoculation (see details in Supporting Information Fig. S8) and means at the 6-h time point were plotted here for clarity.

background of wild-type *P. fluorescens* SBW25. Results of β-galactosidase assays are summarized in Fig. 4 with details shown in Supporting Information Fig. S8. When bacterial cells were shifted from CCR to non-CCR conditions the expression levels of *cbrB*, *crcY* and *crcZ* were elevated, along with a decrease of *crc* gene expression. Significantly, *cbrA* and *hfq* were expressed at similar levels regardless the presence or absence of succinate. These data implicate that CbrB and Crc (but not Hfq) reside at the top of the CCR regulatory hierarchy for the perception of nutrient signals.

Examining fitness conferred by the CCR regulatory system

Having shown that Crc is the direct mediator of CCR in *Pseudomonas*, we took advantage of the *crc* deletion

mutant described above and used it as a CCR⁻ strain to experimentally explore nutrient conditions that require the CCR regulatory system. Briefly, mutant Δ*crc* was mixed 1:1 with a *lacZ*-marked strain of SBW25, and the mixed cells were subject to competitive growth in fresh laboratory medium. Fitness of wild type (CCR⁺) relative to the Δ*crc* mutant (CCR⁻) is expressed as log10 transformed ratios of the Malthusian parameters for each competitor. This results in a fitness value of zero when the two competitors are equally fit, and a positive or negative value when CCR is of advantage or disadvantage, respectively.

First we predicted that the *Pseudomonas* CCR system, as a negative mode of gene regulation, is likely to be beneficial only in environments where the preferred carbon substrate is co-present with the non-preferred carbon substrate; in contrast, it is likely to be disadvantageous if the non-preferred carbon substrate is

Table 2. Fitness of the *crc*, *crcY* and *crcZ* deletion mutants when growing in laboratory media.

	wt/Δ*crc*	Δ*crcYZ*/wt	Δ*crcY*/wt	Δ*crcZ*/wt	Δ*crcY*/Δ*crcZ*
Succinate	−0.075 ± 0.007*	−0.234 ± 0.012*	0.020 ± 0.005	0.012 ± 0.003	−0.004 ± 0.005
Xylose	−0.075 ± 0.003*	−0.630 ± 0.014*	−0.007 ± 0.006	−0.002 ± 0.003	0.012 ± 0.005
Succinate + xylose	0.018 ± 0.003*	−0.172 ± 0.007*	0.002 ± 0.003	−0.022 ± 0.004	0.003 ± 0.003
Glycerol + xylose	−0.050 ± 0.005*	−0.408 ± 0.042*	0.015 ± 0.008	−0.015 ± 0.004	0.013 ± 0.011
LB	0.010 ± 0.003*	−0.114 ± 0.006*	−0.008 ± 0.003	−0.014 ± 0.003	0.015 ± 0.002
Glucose	−0.023 ± 0.006*	−0.704 ± 0.054*	−0.017 ± 0.003	0.003 ± 0.009	0.007 ± 0.003

*Fitness data (means and standard errors of 8 replicates) are log10-transformed ratios of the Malthusian parameters for each competitor, and asterisks indicate significant difference from zero as revealed by the Student's *t*-test ($P < 0.05$). Succinate, glycerol and xylose were provided at the final concentration of 20 mM, and glucose was added at 0.4%. wt stands for wild type.

constantly available as the major carbon source for bacterial growth. Indeed, the wild-type strain was more competitive than the Δ*crc* mutant when growing on succinate + xylose, but less competitive on xylose only (Table 2). Surprisingly, the wild-type strain was disadvantageous over the Δ*crc* mutant when growing in minimal medium with succinate as the sole carbon source. Similar effects were observed for glucose in the M9 medium (Table 2). These data suggest that Crc also inhibits the utilization rate of preferred carbon sources such as succinate and glucose. Glycerol does not produce any detectable CCR effects on *xut* genes expression; thus, it makes sense that addition of glycerol did not restore the fitness cost of CCR for xylose utilization. Interestingly, CCR was advantageous in the complete medium of LB, which had been used as the assay condition for CCR in *P. putida* strains (La Rosa *et al.*, 2015).

Next, we measured the fitness contribution of CCR for cells growing in minimal medium supplemented with xylose (20 mM) and varying concentrations of succinate. The rationale behind the experiment posed that fitness effects contributed via CCR are likely to depend on fluctuating concentrations of succinate. More specifically, CCR confers a growth advantage by use of the preferred carbon sources, but it comes at a price, causing growth slow-down or growth-arrest during periods of metabolic shifts. Therefore, succinate must be present at relatively high concentrations, ensuring that cells receive a positive net fitness gain after shifting their metabolism. Results shown in Fig. 5 indicate a strong positive correlation between succinate concentration and the ecological significance of CCR ($r = 0.967$, $P < 0.0001$). The wild-type strain in which CCR is intact outcompeted the CCR defective strain when succinate was present at concentrations higher than 20 μM; but more significantly, it imposed a fitness burden under low succinate conditions (< 20 μM). Together, our data suggest that the ecological significance of CCR depends on fluctuating concentrations of preferred carbon sources.

Investigating the functional redundancy of CrcY and CrcZ

Data presented above indicate that CrcY and CrcZ play the same roles in the CCR regulatory system, and mutants devoid of *crcY* or *crcZ* grow normally on xylose (Supporting Information Fig. S1A). To assess the possible fitness cost associated with deletion of *crcY* or *crcZ*, strains lacking the two genes were subjected to direct competition with each other (and separately, with wild-type SBW25) in six different laboratory media, including the CCR and non-CCR nutrient conditions. Also included in the fitness assay was a mutant lacking the two ncRNA genes (Δ*crcYZ*). Results revealed no significant difference between Δ*crcY* and Δ*crcZ*, and both mutants were equally fit as the wild type under the tested nutrient conditions (Table 2). As expected, the Δ*crcYZ* mutant was significantly compromised in its
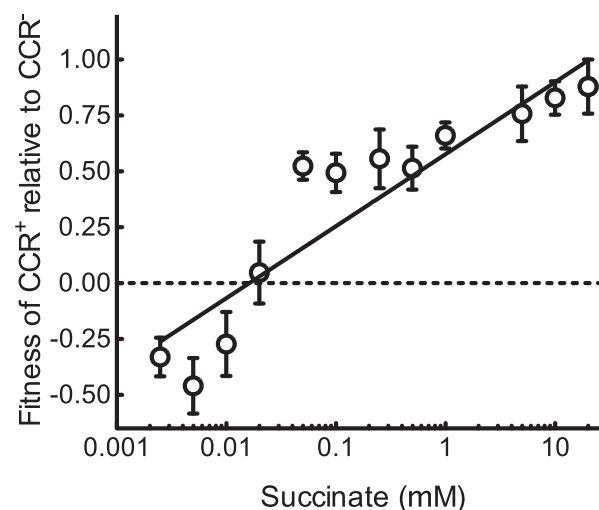

Fig. 5. Fitness of CCR under changing environments of succinate availability. Bacteria were grown in minimal salt medium supplemented with xylose (20 mM) and varying concentrations of succinate, and cells were numerated 12 h after inoculation. Relative fitness was calculated as log10 transformed ratios of the Malthusian parameters for each competitor. Data are means and standard errors of eight independent cultures.
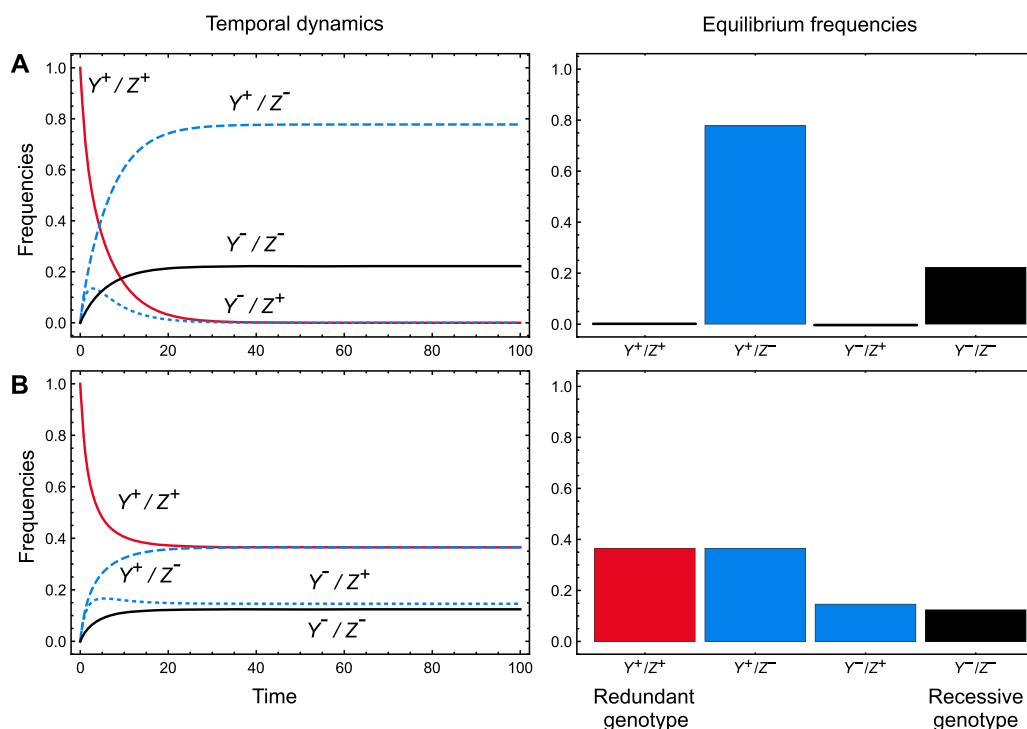
Fig. 6. Predicted temporal dynamics and the final equilibrium frequencies of the four possible genotypes of *crcY* and *crcZ* alleles. Wild-type and mutant alleles are indicated by superscript plus and superscript minus, respectively.

A. True redundancy where one of the knockouts Y^+/Z^- does not result in a fitness reduction as compared to the completely redundant genotype Y^+/Z^+ (f1 = f2 = 1) as compared to the less fit knockout Y^-/Z^+ (f3 = 0.3). In this case for symmetric mutation probability ($QA^->a = QB^->b = 0.2$), the functional knockout increases in frequency. Even if the completely recessive genotype has a lower fitness than the non-functional knockout Y^-/Z^+, it has a higher frequency due to a non-zero fitness and directed mutations.

B. For almost redundancy, the completely redundant genotype Y^+/Z^+ is completely dominant in the fitness space (f1 =1) better than the single knockouts (f2 = 0.6, f3 = 0.3) and certainly better than the recessive genotype (f4 = 0.1). Even for mutation rates directed away from the redundant type ($QA^->a = QB^->b = 0.2$), we see that the redundant genotype is maintained in the population along with the single knockouts.

ability to grow in the six laboratory media, as a result of losing control of the Crc/Hfq-mediated gene repression.

The finding that CrcY and CrcZ are functionally equivalent raises questions as to their maintenance. Theory predicts that one of the two copies will be lost by mutation if there is no selective pressure to maintain both (Zhang, 2012). To help understand if *crcY* and *crcZ* genes are truly redundant, we developed a general deterministic model to predict the dynamic changes of genotype frequency over time for all four possible genotypes, starting from the wild-type strain with two functional copies of *crcY* and *crcZ* (see details in *Experimental procedures*). Consistent with expectations, if *crcY* and *crcZ* contribute equally to fitness, a strain with two functional copies will likely go extinct, with strains harbouring just one copy being maintained over time (Fig. 6A). The redundant copy will likely to be lost due to drift. Furthermore, we found that the two functional copies can only be stably maintained when one-copy genotypes are less fit than the wild type; and moreover, that the one-copy type conferring a lower fitness should have a lower mutation rate. Given that the two genes of *crcY* and *crcZ* are

of similar length, it is most likely that they have the similar mutation rates. The model thus hypothesizes that *crcY* and *crcZ* must have different functions, and consequently, different contributions in different environments.

Discussion

In the present study, we have defined the molecular mechanisms of CCR for the expression of xylose utilization genes in *P. fluorescens* SBW25. Our genetic data show that Crc and Hfq are functionally complementary as both are required for CbrAB-mediated activation of the *xutAFGH* operon. However, only *crc* is transcriptionally responsive to the presence of succinate. Thus our data indicate that Crc is the key CCR regulator in *P. fluorescens* SBW25, but its function requires the RNA-binding property of Hfq. This finding is generally consistent with recent studies in *P. aeruginosa* and *P. putida*, which show that Crc lacks intrinsic RNA-binding properties (Milojevic *et al.*, 2013a; Moreno *et al.*, 2015), but it plays an important role in CCR by enhancing the

specific bindings between Hfq and target mRNAs of certain catabolic genes (Moreno *et al.*, 2015). Hfq is abundant within the cell (Sobrero and Valverde, 2012): hence, kinetics of the CCR system are largely determined by the population of Crc proteins, which are modulated by the P*crc* promoter activity and the antagonistic ncRNAs (CrcY and CrcZ).

Hfq is widespread in prokaryotes including enteric bacteria that do not have post-transcriptional CCR mechanisms (Sun *et al.*, 2002). Hfq participates in a wide range of gene regulations that occur at the post-transcriptional levels, and it is associated with bacterial stress responses and biofilm formation (Sauer, 2013; Arce-Rodriguez *et al.*, 2016). Thus, the newly discovered function of Hfq in CCR control poses a significant question regarding the evolution of the complex CCR system in *Pseudomonas*. From a physiological perspective, it would make more sense if catabolic transcripts were directly targeted by a single protein Crc, without the involvement of the general RNA-binding protein Hfq. Indeed, Crc possesses putative ribonucleotide binding sites, which belong to the EEP (exonuclease/endonuclease/phosphatase) superfamily. Thus, it is reasonable to speculate that in the evolutionary past, CCR in *Pseudomonas* may have been the sole charge of Crc, with benefits arising from evolution or acquisition of Hfq leading to loss of Crc-specific RNA-binding properties. A plausible selective advantage for the recruitment of Hfq is increased stability of mRNAs (Vogel and Luisi, 2011), thus avoiding premature mRNA degradation and ensuring that stalled translation might resume once Crc/Hfq are sequestered by the CbrAB-regulated ncRNAs. To fine-tune gene expression at the translation level it is critically important that catabolic mRNAs be stably maintained when bound with regulatory proteins.

Utilization of nutrients is typically a three-step process that involves detection of the external nutrient signal, followed by efficient uptake and enzymatic breakdown. Data presented here show that CCR operates at mRNAs of all three genetic elements required for xylose utilization (i.e. XutR, XutA and XutFGH) (Liu *et al.*, 2015). Similar regulatory strategies have been described in *P. putida* for the CCR control of genes involved in the utilization of toluene, benzoate and alkanes (Moreno *et al.*, 2010; Hernandez-Arranz *et al.*, 2013). Our measures of the equilibrium dissociation constants (K_d) between Hfq and the five *xut* target sites implicate sequential events of Crc/Hfq binding (and repression) in the presence of succinate: first via mRNAs of XutA (the first enzyme for xylose breakdown) and then via the transcriptional activator XutR, and finally via the ABC-type transporter system XutFGH. The physiological significance for such a sequential repression is unclear, but it is likely a result of natural selection under complex nutrient conditions. It makes sense to slow down

xylose catabolism by reducing the first enzyme of the *xut* pathway, with inhibition being more efficient by first targeting gene translation and then transcription. Once the catabolic rate is reduced, cells need to further diminish expression of transport systems in order to achieve an efficient but balanced cellular metabolism. Nevertheless, targeting both activator and structural genes is likely to ensure a rapid metabolic shift in response to the presence of preferred carbon sources.

The highly conserved CA motif is often used to identify putative CCR target sites and this in turn allows predictions as to whether an uncharacterized pathway might be subject to Crc/Hfq-mediated CCR control (Moreno *et al.*, 2009b; Sonnleitner *et al.*, 2009). CA motifs are typically present in the vicinity of translational start codons, and in many cases they overlap ribosomal binding sites (RBS) at the 5′ end of mRNA transcripts. Thus, it has been proposed that the Crc/Hfq complex inhibits translation initiation through interference with ribosome binding (Rojo, 2010). This is true for the *xutR*, *xutA*, *xutF* and *xutH* genes. Although *xutF* and *xutH* are located within a polycistronic mRNA of four genes, initiation of translation is likely subject to inhibition by Crc/Hfq. Significantly, we identified an additional functional Crc/Hfq binding site (*xutF2*) located in the internal coding region of *xutF*, suggesting that Crc/Hfq can also inhibit translation elongation. Together, these data suggest that CCR in *Pseudomonas* is regulated more tightly than previously thought: the search for putative CCR targets ought not be restricted to regions of translational start sites.

A remarkable feature of the proposed CCR model in *P. fluorescens* SBW25 is the involvement of two ncRNAs – CrcY and CrcZ – in modulating the Crc/Hfq activities. We show that *crcY* and *crcZ* are genetically interchangeable. Both are regulated by the CbrAB two-component regulatory system in a σ^{54}-dependent manner. Significantly, deletion of either *crcY* or *crcZ* did not cause any detectable fitness reduction in laboratory media, including CCR and non-CCR nutrient conditions. Apparently, one copy is sufficient for the CCR function. This is a fact evident in the genomes of *P. aeruginosa* and *P. mendocina*, which contain a single copy (of CrcZ). The number of CCR ncRNAs per genome appears to be a species-specific feature of *Pseudomonas*. For example, *P. putida* strains harbour two copies of ncRNAs (CrcY and CrcZ), but strains of the plant pathogen *P. syringae* have three copies, namely, CrcY, CrcZ and CrcX (Filiatrault *et al.*, 2013). Intriguingly, the *crcY* homologue of *P. syringae* pv. *tomato* DC3000 is disrupted by an insertion element, and mutants devoid of *crcZ* or *crcX* grow normally in laboratory media (Filiatrault *et al.*, 2010). All empirical evidence to date suggests that the multiple copies of ncRNAs are subject to CbrAB regulation despite variation in the number of nucleotides between two conserved palindromic

motifs (TGTTAC-Nx-GTAACA) for CbrB binding (Sonnleitner *et al.*, 2009; Moreno *et al.*, 2012; Garcia-Maurino *et al.*, 2013; Filiatrault *et al.*, 2013).

Genetic redundancy is a frequently encountered property of biological systems, and may confer both robustness and evolvability to living organisms (Fares, 2015). However, it is challenging to understand how redundant genes can be evolutionarily maintained when there is no obvious selective pressure. It is not uncommon that multiple copies of ncRNAs play the same regulatory role in bacterial gene expression. For example, sequestration of the RNA-binding protein RsmA in the Gac regulon involves two ncRNAs (RsmY and RsmZ) in *P. aeruginosa*, three ncRNAs (RsmX, RsmY and RsmZ) in *P. fluorescens*, and a total of seven ncRNAs in *P. syringae* pv. *tomato* DC3000 (five copies of RsmX plus RsmY and RsmZ) (Lapouge *et al.*, 2008; Brencic *et al.*, 2009; Moll *et al.*, 2010).

In this work, we developed a deterministic model and explored the evolutionary conditions for *crcY* and *crcZ* co-existence. It should be noted that, with a slight modification, this model also applies for the analysis of three or more redundant genes. The data allow us to reject the hypothesis that *crcY* and *crcZ* are truly redundant. Despite the fact that *crcY* and *crcZ* are interchangeable for bacterial growth in the tested laboratory media, they are predicted to have different biological functions and confer distinct advantages or disadvantages under specific environmental conditions, e.g. on plant surfaces. More specifically, *crcY* and *crcZ* may be differentially involved in other yet unknown regulatory effects beyond CCR, particularly those involving Hfq. It is also possible that *crcY* and *crcZ* differ in their own regulation as evidenced in *P. putida* where it has been shown that *crcY* is additionally controlled by a CbrAB-independent promoter; and consequently, this ncRNA can be generated from RNA processing of a longer transcript formed together with the two preceding genes *PP3539* and *mvaB* (Garcia-Maurino *et al.*, 2013). Interestingly, Moreno *et al.* (2012) found that deletion of one of the two ncRNAs (*crcY* or *crcZ*) leads to a compensatory increase of the remaining ncRNA. This suggests the existence of positive feedback mechanisms for the control of the CCR ncRNA pool concentration. Together, our results call for further investigations into the functional difference between *crcY* and *crcZ*, particularly the modes of individual regulation. An alternate possibility is that multiple copies of the ncRNAs serve exactly the same function with important regulatory effects requiring levels of ncRNAs beyond that achievable by transcription from a single promoter under certain environmental conditions.

CCR is a mechanism that allows bacteria to preferentially utilize one specific carbon substrate over another when they are co-present in the environment (Deutscher, 2008). However, this classical view derived from enteric bacteria appears not to apply for CCR in pseudomonads. Strains of *Pseudomonas* are metabolically versatile but inhabit environments that are nutritionally complex and highly competitive (Palleroni, 2005). In previous work, we proposed a gluttonous strategy for nutrient acquisition by pseudomonads, on the basis of the fact that CbrAB is capable of ensuring activity of *hut* across a range of C/N ratios (Zhang and Rainey, 2008). As a competitive opportunist, the primary goal of a *Pseudomonas* strain is to bring into the cell as much of any available resource as quickly as possible, ensuring that competitors are deprived of resources. However, the gluttonous approach poses a significant challenge for bacterial cells to maintain metabolic balance and achieve the maximum possible growth rate, while allaying deleterious effects of gluttony, including build up of toxic intermediates. To overcome this metabolic challenge, it appears that *Pseudomonas* has evolved post-transcriptional CCR mechanisms: the primary physiological role of CCR being to coordinate the expression of catabolic genes to ensure a balanced intracellular metabolism. Similar to enteric bacteria, a nutrient preference might be observed in laboratory assays for pseudomonads (Collier *et al.*, 1996; Moreno *et al.*, 2009a; La Rosa *et al.*, 2016), however, this does not necessarily mean that CCR has evolved for preferential nutrient utilization – rather, it may govern different degrees of repression for all available substrates on the basis of their quality and quantity.

The primary role of CCR in maintaining metabolic balance is consistent with the finding that CCR is advantageous in a minimal medium containing both succinate and xylose (and also in complete LB medium). However, there is a fitness cost associated with CCR when *P. fluorescens* SBW25 is grown on either succinate or xylose as the sole carbon source. Additionally, succinate does not abolish the expression of *xut* genes as expected of a fully functioning CCR system for preferential nutrient acquisition (Fig. 2). Influences of CCR on carbon fluxes have been evidenced by metabolomics studies in *P. putida* and *P. aeruginosa* (La Rosa *et al.*, 2015; La Rosa *et al.*, 2016). For example, inactivation of *crc* causes excretion of acetate and pyruvate when bacteria were grown exponentially in complete LB medium, and these valuable metabolites are later consumed when bacterial growth is slowed down in stationary phase, demonstrating an important role of Crc in balanced bacterial growth (La Rosa *et al.*, 2016).

The natural habitat of *P. fluorescens* SBW25 is the plant surface – a nutritionally complex environment (Silby *et al.*, 2009). During the process of plant development the composition and relative abundance of nutritional substrates are subject to dynamic changes in a spatially and temporally dependent manner. Thus, plant-colonizing

bacteria continuously alter patterns of gene expression, particularly those involved in nutrition acquisition. A genome-wide search for genes whose expression is elevated during plant colonization has been performed on sugar beet seedlings using promoter-trapping techniques (Gal *et al.*, 2003; Giddens *et al.*, 2007). This led to the identification of 139 plant-inducible genes, including *dctA* for succinate uptake and *xutA* for xylose catabolism (Rainey, 1999). These data strongly implicate succinate and xylose as two frequently encountered carbon substrates *in planta*. The fitness data presented here further suggest that succinate may fluctuate at relatively high concentrations, as presence of CCR confers a selective disadvantage when succinate is co-present at low concentrations with xylose.

Finally, it is interesting to note that the Crc/Hfq system is involved in the regulation of succinate acquisition genes in *P. aeruginosa*, depending on the concentrations of external succinate (Valentini and Lapouge, 2013). Specifically, *P. aeruginosa* PAO1 possesses two succinate-specific transporters DctA and DctPQM, which are responsible for succinate uptake at high (mM range) and low (μM range) concentrations, respectively (Valentini *et al.*, 2011). These two systems are differentially regulated by Crc/Hfq when succinate is present at high concentrations. While Crc represses the expression of DctPQM, it enhances the expression of DctA through the effects of the transcriptional repressor DctR. In *P. fluorescens* SBW25, a *dctR* homologue is present at the *dctA* locus, but it does not contain the putative CA motif as found in *P. aeruginosa* PAO1, suggesting that Crc/Hfq is not directly involved in the CCR control of *dctA* expression. Moreover, the *dctPQM* homologues (*pflu3468-pflu3470*) can catalyse succinate uptake, but they play no role in succinate utilization, as the genes are transcriptionally unresponsive to succinate in the medium (X.X. Zhang, unpublished). Together, the data suggest that the utilization of succinate is also subject to CCR control, which in *P. fluorescens* SBW25 may occur in a complex Crc/Hfq-independent manner.

Experimental procedures

Bacterial strains and growth conditions

A summary of bacterial strains and plasmids used in this work is provided in Table 1. The *E. coli* strain DH5αλ_{pir} was used for gene cloning and subsequent conjugation into *Pseudomonas*. The ancestral *P. fluorescens* SBW25 is a plasmid-free, non-pathogenic, rRNA group 1 fluorescent *Pseudomonas*, which was isolated in 1989 from the leaf surface of a sugar beet plant grown at the University of Oxford farm, Wytham, Oxford, UK (Rainey and Bailey, 1996). *P. fluorescens* SBW25 and its derived mutants were generally cultivated at 28°C in Luria-Bertani medium (LB) and also in the minimal M9 medium with glucose and

ammonium as the sole carbon and nitrogen sources, respectively. When *P. fluorescens* strains were grown in M9 salts medium (MSM), each carbon source was supplemented at the final concentration of 20 mM except where indicated. Growth kinetics were examined in a 96-well plate using a Synergy 2 plate reader equipped with the Gen5 software (BioTek Instruments). To ensure that all strains in comparison were physiologically equivalent, bacteria stored in a −80°C freezer were first inoculated into LB broth, and cells in the overnight cultures were washed once and resuspended in MSM broth. After starvation for 2 h at 28°C, 2 μl was inoculated into 200 μl of the tested medium per well. The plate was moderately shaken for 10 s prior to each read. Absorbance at 450 nm was measured every 5 min over a period of either 48 or 72 h, and data from 5 h intervals are plotted for clarity.

Random and site-directed mutagenesis analysis

Standard protocols were used for the preparation of plasmid DNAs, restriction endonuclease digestion, ligation and transformation. The CCR genes were cloned from the genomic DNA of *P. fluorescens* SBW25 by PCR using specifically designed primers. All PCR reactions were performed using *Taq* DNA polymerase from Invitrogen (Auckland, New Zealand). Oligonucleotide primers used in this work are listed in Supporting Information Table S1. The PCR products were first cloned into pCR8/GW/TOPO by using the TA cloning kit purchased from Invitrogen (Auckland), and then subjected to DNA sequencing at Macrogen Inc. Once sequence identity was confirmed, the DNA insert was subcloned into an appropriate destination vector such as pUIC3 for gene mutation or a mini-Tn7 vector for the construction of a *lacZ* reporter fusion. Gene mutation *in vivo* was achieved as previously described using a combination of SOE-PCR (splicing by overlapping extension using the polymerase chain reaction [Horton *et al.*, 1989]) and a two-step allelic-exchange strategy with the suicide-integration vector pUIC3 (Rainey, 1999). When necessary, a previous described procedure of D-cycloserine enrichment was used to select for the desired double crossover mutants (Zhang and Rainey, 2007).

The transposon (Tn) used in this study was IS-Ω-Km/hah, which is a modified version of IS*phoA*/hah with *phoA* and the chloramphenicol resistance (Cm^r) gene being replaced by an Ω-Km cassette (Giddens *et al.*, 2007). Conjugation was performed on a filter in an LB agar plate as previously described (Zhang *et al.*, 2015). Briefly, *P. fluorescens* cells were subjected to heat shock at 45°C for 20 min before being mixed 1:1 with *E. coli* S17–1λ*pir* (pSCR001). pSCR001 is the plasmid carrying IS-Ω-Km/hah. The conjugation mix was then incubated at 28°C for 4 h. Next, cells on the filter were re-suspended in 1 ml sterile water and dilute-plated onto selective plates of MSM supplemented with xylose as the sole carbon source and nitrofurantoin (100 μg ml^{-1}, to counter-select *E. coli*) and kanamycin (Km, 100 μg ml^{-1}). Location of the Tn was mapped to the genome by sequencing the DNA fragments obtained by arbitrarily primed PCR (AP-PCR) using a protocol previously described by Manoil (2000).

Assays for gene expression and bacterial fitness

To construct a transcriptional *lacZ* fusion the promoter region (∼800 bp) was cloned into either pUIC3 or pUC18-mini-Tn7-Gm-*lacZ*. The resultant pUIC3 recombinant plasmid was introduced into *P. fluorescens* through conjugation with the help of pRK2013, and the *lacZ* reporter was integrated into the chromosome via homologous recombination of the cloned DNA fragment. In the contrast, the recombinant plasmid of pUC18-mini-Tn7-Gm-*lacZ* was electroporated into *P. fluorescens* together with pUX-BF13, and the mini-Tn7 element carrying the *lacZ* reporter fusion was integrated into the unique Tn7 site located downstream of *glmS* (Choi *et al.*, 2005). Translational *lacZ* fusions were made similarly in pXY2, a modified version of pUC18-mini-Tn7-Gm-*lacZ* (Liu *et al.*, 2014). β-Galactosidase activity was assayed using 4-methylumbelliferyl-b-D-galactoside (4MUG) as the enzymatic substrate, and the fluorescent product, 7-hydroxy-4-methylcoumarin (4MU), was detected at 460 nm after excision at 365 nm using a Synergy 2 plate reader (BioTek Instruments). Enzyme activity was expressed as the amount of 4MU (μM) produced per min per cell (A_{600}).

A neutral *lacZ*-marked strain of wild-type *P. fluorescens* SBW25 was used to assay the possible fitness cost associated with mutation of CCR regulators. In the case of direct competition between Δ*crcY* and Δ*crcZ*, the Δ*crcY* mutant was marked with a promoterless *lacZ* derived from the plasmid vector pUC18-mini-Tn7-Gm-*lacZ*. Bacteria were first inoculated into LB broth using cells stored at −80°C. Overnight cultures were washed once with MSM buffer and subjected to 2 h starvation at 28°C, ensuring that the two competitors were at comparable physiological states. The cells were then mixed at 1:1 and inoculated into the tested medium by 1000-times dilution. Population densities (N_i) at time $t = 0$ and $t = T$ were used to calculate the Malthusian parameter (m_i) for each competitor, which is the average rate of increase: $m_i = \ln[N_i(T)/N_i(0)]$. Relative fitness is expressed as the log10 transformed ratios of the two competitors: $r_{ij} = \log10(m_i/m_j)$, resulting in a fitness of zero when the two strains equally fit.

Electrophoretic mobility shift assays

The coding regions of Crc and Hfq were amplified by PCR from the genomic DNA of *P. fluorescens* SBW25 with the integration of six histidine residues at the C- and N-terminal, respectively (Supporting Information Table S1). The PCR product was first cloned into pCR8/GW/TOPO and subjected to DNA sequencing. Next, the error-free insert was subcloned into the protein expression vector pTrc99A (Amann *et al.*, 1988). The recombinant plasmids pTrc99A-*crc* and pTrc99A-*hfq* were transformed into *E. coli* BL21(DE3) (Studier and Moffatt, 1986), and 1 mM IPTG was added to *E. coli* culture at mid-log phase (A_{600}, ∼0.6) to induce protein expression. The His$_6$-tagged Crc and Hfq proteins were purified using TALON metal affinity resin (Clontech Laboratories Inc.) according to the manufacturer's protocol. Crc$_{His6}$ was subjected to two successive regular washes with 20 mM and 40 mM imidazole. For the purification of Hfq$_{His6}$, an additional washing step with a higher concentration of imidazole (70 mM) was used to eliminate the effects of residual

Hfq$_{E.coli}$. The efficacy of Hfq$_{E.coli}$ elimination was demonstrated in a control study using the transcriptional regulator HutC$_{His6}$, which was also expressed in pTrc99A and purified in parallel with Hfq$_{His6}$ (Supporting Information Fig. S9).

RNA probes for EMSA analysis were obtained by *in vitro* transcription using the T7 Quick High Yield RNA Synthesis Kit purchased from the New England Biolabs Ltd. The template DNA was plasmid pCR8/GW/TOPO containing the corresponding DNA, which was obtained by PCR with T7 promoter sequence being integrated in the forward primer (Supporting Information Table S1). RNA probes were end-labelled with biotin using Pierce™ RNA 3′ End Biotinylation Kit (Thermo Fisher Scientific), and were further purified through a denaturing polyacrylamide (6%) and urea (7 M) gel. The protein-RNA interaction was assayed in a 20 μl reaction containing 0.1 μM biotin-labeled probe and varying concentrations of purified Crc or Hfq. The binding buffer was composed of 10 mM HEPES (pH 7.9), 35 mM KCl and 2 mM MgCl$_2$. The reaction also contained 1 μg unrelated yeast tRNA as a control agent for nonspecific binding. After incubation at room temperature for 30 min, the RNA probes were separated on a 6% non-denaturing polyacrylamide gel in 0.5x TBE buffer at 4°C (Sambrook *et al.*, 1989). RNAs in the gel were then transferred by electroblotting to positively charged nylon membrane (Whatman® Nytran™ SuPer-Charge, Sigma-Aldrich). RNA fragments were immobilized by baking at 80°C for 30 min, and they were finally detected using the Pierce's LightShift™ chemiluminescent EMSA kit (Thermo Fisher Scientific, Auckland) following the manufacturer's recommendation. The image was visualized using the Luminescent Image Analyzer LAS-4000 system equipped with the Image Reader LAS-4000 software (Fujifilm).

Mathematical modelling

The model of genetic redundancy was developed by taking both mutation rate and organism fitness into consideration. We assume a haploid organism with clonal inheritance, no recombination and unidirectional mutation. We started with two different alleles *A* and *B*, which will have a total of four possible genotypes *AB*, *Ab*, *aB* or *ab* for an organism. Capital versions represent the functional alleles, whereas the lower cases are the non-functional versions. The frequencies of these genotypes in a population are given by $x1$, $x2$, $x3$ and $x4$. Directional mutations from the functional to the non-functional variants are given by μ_a and μ_b (assumed to be symmetrical) captured in the mutational matrix *Q*.

$$Q = \begin{array}{c} \\ AB \\ Ab \\ aB \\ ab \end{array} \begin{array}{cccc} AB & Ab & aB & ab \end{array} \\ \begin{pmatrix} (1-\mu_a)(1-\mu_b) & \mu_b & \mu_a & \mu_a\mu_b \\ 0 & 1-\mu_a & 0 & \mu_a \\ 0 & 0 & 1-\mu_b & \mu_b \\ 0 & 0 & 0 & 1 \end{pmatrix} \quad (1)$$

The dynamics of the genotype frequencies are then captured by the following four difference equations.

$$\bar{f}x_1' = (x_1 q_{AB \to AB} f_{AB} + x_2 q_{Ab \to AB} f_{Ab} \\ + x_3 q_{aB \to AB} f_{aB} + x_4 q_{ab \to AB} f_{ab}) \tag{2}$$

$$\bar{f}x_2' = (x_1 q_{AB \to Ab} f_{AB} + x_2 q_{Ab \to Ab} f_{Ab} \\ + x_3 q_{aB \to Ab} f_{aB} + x_4 q_{ab \to Ab} f_{ab}) \tag{3}$$

$$\bar{f}x_3' = (x_1 q_{AB \to aB} f_{AB} + x_2 q_{Ab \to aB} f_{Ab} \\ + x_3 q_{aB \to aB} f_{aB} + x_4 q_{ab \to aB} f_{ab}) \tag{4}$$

$$\bar{f}x_4' = (x_1 q_{AB \to ab} f_{AB} + x_2 q_{Ab \to ab} f_{Ab} \\ + x_3 q_{aB \to ab} f_{aB} + x_4 q_{ab \to ab} f_{ab}) \tag{5}$$

where $\bar{f}$ is such that $x1 + x2 + x3 + x4 = 1$.

Fitness of each genotype is a crucial factor. We modulate these to represent the different types of redundancies (Nowak *et al.*, 1997). In the case of true redundancy a knockout mutant of one of the redundant alleles (Thomas, 1993; Brookfield, 1997), i.e. *Ab* or *aB* can still act fully as AB, thus, $f_{AB} = f_{Ab} = f_{aB}$. Generic redundancy is the case when an *AB* individual is only occasionally better than an *Ab* or *aB* individual. Almost redundancy means that the redundant genotype AB is always slightly better than any genotype where one of the redundant genes has been knocked out (Thomas, 1993).

Simplifying the expressions and in continuous time we have,

$$\dot{x}_i = \sum_{j=1}^{4} x_j f_j q_{j \to i} - x_i \bar{f} \tag{6}$$

which is a set of four coupled quasispecies equations. An equilibrium solution to a given set of fitness values and mutation rates is given by the eigenvector corresponding to the largest eigenvalue of this system of equations (Nowak, 1992).

Acknowledgements

References

Amann, E., Ochs, B., and Abel, K.J. (1988) Tightly regulated tac promoter vectors useful for the expression of unfused and fused proteins in *Escherichia coli*. *Gene* **69**: 301–315.

Arce-Rodriguez, A., Calles, B., Nikel, P.I., and de Lorenzo, V. (2016) The RNA chaperone Hfq enables the environmental stress tolerance super-phenotype of *Pseudomonas putida*. *Environ Microbiol* **18**: 3309–3326.

Bailey, M.J., Lilley, A.K., Thompson, I.P., Rainey, P.B., and Ellis, R.J. (1995) Site directed chromosomal marking of a fluorescent pseudomonad isolated from the phytosphere of sugar beet; stability and potential for marker gene transfer. *Mol Ecol* **4**: 755–763.

Bao, Y., Lies, D.P., Fu, H., and Roberts, G.P. (1991) An improved Tn7-based system for the single-copy insertion of cloned genes into chromosomes of Gram-negative bacteria. *Gene* **109**: 167–168.

Brencic, A., McFarland, K.A., McManus, H.R., Castang, S., Mogno, I., Dove, S.L., and Lory, S. (2009) Th GacS/GacA signal transduction system of *Pseudomonas aeruginosa* acts exclusively through its control over the transcription of the RsmY and RsmZ regulatory small RNAs. *Mol Microbiol* **73**: 434–445.

Brookfield, J.F.Y. (1997) Genetic redundancy. *Adv Genet* **36**: 137–155.

Choi, K.H., Gaynor, J.B., White, K.G., Lopez, C., Bosio, C.M., Karkhoff-Schweizer, R.R., and Schweizer, H.P. (2005) A Tn7-based broad-range bacterial cloning and expression system. *Nat Methods* **2**: 443–448.

Collier, D.N., Hager, P.W., and Phibbs, P.V., Jr., (1996) Catabolite repression control in the pseudomonads. *Res Microbiol* **147**: 551–561.

Dakora, F.D., and Phillips, D.A. (2002) Root exudates as mediators of mineral acquisition in low-nutrient environments. *Plant Soil* **245**: 35–47.

Deutscher, J. (2008) The mechanisms of carbon catabolite repression in bacteria. *Curr Opin Microbiol* **11**: 87–93.

Ditta, G., Stanfield, S., Corbin, D., and Helinski, D.R. (1980) Broad host range DNA cloning system for Gram-negative bacteria: construction of a gene bank of *Rhizobium meliloti*. *Proc Natl Acad Sci USA* **77**: 7347–7351.

Fares, M.A. (2015) The origins of mutational robustness. *Trends Genet* **31**: 373–381.

Filiatrault, M.J., Stodghill, P.V., Bronstein, P.A., Moll, S., Lindeberg, M., Grills, G., *et al.* (2010) Transcriptome analysis of *Pseudomonas syringae* identifies new genes, noncoding RNAs, and antisense activity. *J Bacteriol* **192**: 2359–2372.

Filiatrault, M.J., Stodghill, P.V., Wilson, J., Butcher, B.G., Chen, H.R., Myers, C.R., and Cartinhour, S.W. (2013) CrcZ and CrcX regulate carbon source utilization in *Pseudomonas syringae* pathovar *tomato* strain DC3000. *RNA Biol* **10**: 245–255.

Gal, M., Preston, G.M., Massey, R.C., Spiers, A.J., and Rainey, P.B. (2003) Genes encoding a cellulosic polymer contribute toward the ecological success of *Pseudomonas fluorescens* SBW25 on plant surfaces. *Mol Ecol* **12**: 3109–3121.

Garcia-Maurino, S.M., Perez-Martinez, I., Amador, C.I., Canosa, I., and Santero, E. (2013) Transcriptional activation of the CrcZ and CrcY regulatory RNAs by the CbrB response regulator in *Pseudomonas putida*. *Mol Microbiol* **89**: 189–205.

Giddens, S.R., Jackson, R.W., Moon, C.D., Jacobs, M.A., Zhang, X.X., Gehrig, S.M., and Rainey, P.B. (2007) Mutational activation of niche-specific genes provides insight into regulatory networks and bacterial function in a complex environment. *Proc Natl Acad Sci USA* **104**: 18247–18252.

Goerke, B., and Stulke, J. (2008) Carbon catabolite repression in bacteria: many ways to make the most out of nutrients. *Nat Rev Microbiol* **6**: 613–624.

Hernandez-Arranz, S., Moreno, R., and Rojo, F. (2013) The translational repressor Crc controls the *Pseudomonas putida* benzoate and alkane catabolic pathways using a multi-tier regulation strategy. *Environ Microbiol* **15**: 227–241.

Hester, K.L., Lehman, J., Najar, F., Song, L., Roe, B.A., MacGregor, C.H., *et al*. (2000) Crc is involved in catabolite repression control of the *bkd* operons of *Pseudomonas putida* and *Pseudomonas aeruginosa*. *J Bacteriol* **182**: 1144–1149.

Horton, R.M., Hunt, H.D., Ho, S.N., Pullen, J.K., and Pease, L.R. (1989) Engineering hybrid genes without the use of restriction enzymes: gene splicing by overlap extension. *Gene* **77**: 61–68.

La Rosa, R., Behrends, V., Williams, H.D., Bundy, J.G., and Rojo, F. (2016) Influence of the Crc regulator on the hierarchical use of carbon sources from a complete medium in *Pseudomonas*. *Environ Microbiol* **18**: 807–818.

La Rosa, R., Nogales, J., and Rojo, F. (2015) The Crc/CrcZ-CrcY global regulatory system helps the integration of gluconeogenic and glycolytic metabolism in *Pseudomonas putida*. *Environ Microbiol* **17**: 3362–3378.

Lapouge, K., Schubert, M., Allain, F.H.T., and Haas, D. (2008) Gac/Rsm signal transduction pathway of gammaproteobacteria: from RNA recognition to regulation of social behaviour. *Mol Microbiol* **67**: 241–253.

Liu, Y., Rainey, P.B., and Zhang, X.X. (2014) Mini-Tn7 vectors for studying post-transcriptional gene expression in *Pseudomonas*. *J Microbiol Methods* **107**: 182–185.

Liu, Y., Rainey, P.B., and Zhang, X.X. (2015) Molecular mechanisms of xylose utilization by *Pseudomonas fluorescens*: overlapping genetic responses to xylose, xylulose, ribose and mannitol. *Mol Microbiol* **98**: 553–570.

Lu, C.D., Winteler, H., Abdelal, A., and Haas, D. (1999) The ArgR regulatory protein, a helper to the anaerobic regulator ANR during transcriptional activation of the *arcD* promoter in *Pseudomonas aeruginosa*. *J Bacteriol* **181**: 2459–2464.

MacGregor, C.H., Arora, S.K., Hager, P.W., Dail, M.B., and Phibbs, P.V. Jr., (1996) The nucleotide sequence of the *Pseudomonas aeruginosa pyrE-crc-rph* region and the purification of the *crc* gene product. *J Bacteriol* **178**: 5627–5635.

MacGregor, C.H., Wolff, J.A., Arora, S.K., and Phibbs, P.V. Jr., (1991) Cloning of a catabolite repression control (*crc*) gene from *Pseudomonas aeruginosa*, expression of the gene in *Escherichia coli*, and identification of the gene product in *Pseudomonas aeruginosa*. *J Bacteriol* **173**: 7204–7212.

Manoil, C. (2000) Tagging exported proteins using *Escherichia coli* alkaline phosphatase gene fusions. *Methods Enzymol* **326**: 35–47.

Milojevic, T., Grishkovskaya, I., Sonnleitner, E., Djinovic-Carugo, K., and Bläsi, U. (2013a) The *Pseudomonas aeruginosa* catabolite repression control protein Crc is devoid of RNA binding activity. *PLoS One* **8**: e64609.

Milojevic, T., Sonnleitner, E., Romeo, A., Djinovic-Carugo, K., and Bläsi, U. (2013b) False positive RNA binding activities after Ni-affinity purification from *Escherichia coli*. *RNA Biol* **10**: 1066–1069.

Moll, S., Schneider, D.J., Stodghill, P., Myers, C.R., Cartinhour, S.W., and Filiatrault, M.J. (2010) Construction of an *rsmX* co-variance model and identification of five *rsmX* non-coding RNAs in *Pseudomonas syringae* pv. *tomato* DC3000. *RNA Biol* **7**: 508–516.

Moreno, R., Fonseca, P., and Rojo, F. (2010) The Crc global regulator inhibits the *Pseudomonas putida* pWW0 toluene/xylene assimilation pathway by repressing the translation of regulatory and structural genes. *J Biol Chem* **285**: 24412–24419.

Moreno, R., Fonseca, P., and Rojo, F. (2012) Two small RNAs, CrcY and CrcZ, act in concert to sequester the Crc global regulator in *Pseudomonas putida*, modulating catabolite repression. *Mol Microbiol* **83**: 24–40.

Moreno, R., Hernandez-Arranz, S., La Rosa, R., Yuste, L., Madhushani, A., Shingler, V., and Rojo, F. (2015) The Crc and Hfq proteins of *Pseudomonas putida* cooperate in catabolite repression and formation of ribonucleic acid complexes with specific target motifs. *Environ Microbiol* **17**: 105–118.

Moreno, R., Martinez-Gomariz, M., Yuste, L., Gil, C., and Rojo, F. (2009a) The *Pseudomonas putida* Crc global regulator controls the hierarchical assimilation of amino acids in a complete medium: evidence from proteomic and genomic analyses. *Proteomics* **9**: 2910–2928.

Moreno, R., Marzi, S., Romby, P., and Rojo, F. (2009b) The Crc global regulator binds to an unpaired A-rich motif at the *Pseudomonas putida alkS* mRNA coding sequence and inhibits translation initiation. *Nucleic Acids Res* **37**: 7678–7690.

Nowak, M.A. (1992) What is a quasispecies?. *Trends Ecol Evol* **7**: 118–121.

Nowak, M.A., Boerlijst, M.C., Cooke, J., and Smith, J.M. (1997) Evolution of genetic redundancy. *Nature* **388**: 167–171.

Palleroni, N.J. (2005) Genus I. *Pseudomonas*. In *Bergey's Manual of Systematic Bacteriology*. Brenner, D.J., Krieg, N.R., Staley, J.T., and Garrity, G.M. (eds). New York: Springer, pp. 323–379.

Phillips, A.T., and Mulfinger, L.M. (1981) Cyclic adenosine 3',5'-monophosphate levels in *Pseudomonas putida* and *Pseudomonas aeruginosa* during induction and carbon catabolite repression of histidase synthesis. *J Bacteriol* **145**: 1286–1292.

Rainey, P.B. (1999) Adaptation of *Pseudomonas fluorescens* to the plant rhizosphere. *Environ Microbiol* **1**: 243–257.

Rainey, P.B., and Bailey, M.J. (1996) Physical and genetic map of the *Pseudomonas fluorescens* SBW25 chromosome. *Mol Microbiol* **19**: 521–533.

Rojo, F. (2010) Carbon catabolite repression in *Pseudomonas*: optimizing metabolic versatility and interactions with the environment. *FEMS Microbiol Rev* **34**: 658–684.

Ruiz-Manzano, A., Yuste, L., and Rojo, F. (2005) Levels and activity of the *Pseudomonas putida* global regulatory protein Crc vary according to growth conditions. *J Bacteriol* **187**: 3678–3686.

Sambrook, J., Fritsch, E.F., and Maniatis, T., (1989) *Molecular Cloning: A Laboratory Manual*. Cold Spring Harbor Laboratory Press, New York, USA.

Sauer, E. (2013) Structure and RNA-binding properties of the bacterial LSm protein Hfq. *RNA Biol* **10**: 610–618.

Shallom, D., and Shoham, Y. (2003) Microbial hemicellulases. *Curr Opin Microbiol* **6**: 219–228.

Silby, M.W., Cerdeno-Tarraga, A.M., Vernikos, G.S., Giddens, S.R., Jackson, R.W., Preston, G.M., *et al.* (2009) Genomic and genetic analyses of diversity and plant interactions of *Pseudomonas fluorescens. Genome Biol* **10**: R51.

Sobrero, P., and Valverde, C. (2012) The bacterial protein Hfq: much more than a mere RNA-binding factor. *Crit Rev Microbiol* **38**: 276–299.

Sonnleitner, E., Abdou, L., and Haas, D. (2009) Small RNA as global regulator of carbon catabolite repression in *Pseudomonas aeruginosa. Proc Natl Acad Sci USA* **106**: 21866–21871.

Studier, F.W., and Moffatt, B.A. (1986) Use of bacteriophage T7 RNA polymerase to direct selective high-level expression of cloned genes. *J Mol Biol* **189**: 113–130.

Suh, S.J., Runyen-Janecky, L.J., Maleniak, T.C., Hager, P., MacGregor, C.H., Zielinski-Mozny, N.A., Phibbs, P.V., Jr., *et al.* (2002) Effect of *vfr* mutation on global gene expression and catabolite repression control of *Pseudomonas aeruginosa. Microbiology* **148**: 1561–1569.

Sun, X., Zhulin, I., and Wartell, R.M. (2002) Predicted structure and phyletic distribution of the RNA-binding protein Hfq. *Nucleic Acids Res* **30**: 3662–3671.

Thomas, J.H. (1993) Thinking about genetic redundancy. *Trends Genet* **9**: 395–399.

Valentini, M., and Lapouge, K. (2013) Catabolite repression in *Pseudomonas aeruginosa* PAO1 regulates the uptake of C_4-dicarboxylates depending on succinate concentration. *Environ Microbiol* **15**: 1707–1716.

Valentini, M., Storelli, N., and Lapouge, K. (2011) Identification of C_4-dicarboxylate transport systems in *Pseudomonas aeruginosa* PAO1. *J Bacteriol* **193**: 4307–4316.

Vogel, J., and Luisi, B.F. (2011) Hfq and its constellation of RNA. *Nat Rev Microbiol* **9**: 578–589.

Zhang, J.Z. (2012) Genetic redundancies and their evolutionary maintenance. *Adv Exp Med Biol* **751**: 279–300.

Zhang, X.X., Gauntlett, J.C., Oldenburg, D.G., Cook, G.M., and Rainey, P.B. (2015) Role of the transporter-like sensor kinase CbrA in histidine uptake and signal transduction. *J Bacteriol* **197**: 2867–2878.

Zhang, X.X., Liu, Y.H., and Rainey, P.B. (2010) CbrAB-dependent regulation of *pcnB*, a poly(A) polymerase gene involved in polyadenylation of RNA in *Pseudomonas fluorescens. Environ Microbiol* **12**: 1674–1683.

Zhang, X.X., and Rainey, P.B. (2007) Genetic analysis of the histidine utilization (*hut*) genes in *Pseudomonas fluorescens* SBW25. *Genetics* **176**: 2165–2176.

Zhang, X.X., and Rainey, P.B. (2008) Dual involvement of CbrAB and NtrBC in the regulation of histidine utilization in *Pseudomonas fluorescens* SBW25. *Genetics* **178**: 185–195.

Supporting information

Additional supporting information may be found in the online version of this article at the publisher's web-site.